Journal of Power Sources 265 (2014) 36–39

Contents lists available at ScienceDirect

Journal of Power Sources

journal homepage: www.elsevier.com/locate/jpowsour

Short communication

The Na[FSA]–[C_2C_1im][FSA] ($C_2C_1im^+$:1-ethyl-3-methylimidazolium and FSA^-:bis(fluorosulfonyl)amide) ionic liquid electrolytes for sodium secondary batteries

Kazuhiko Matsumoto [a,b], Takafumi Hosokawa [a], Toshiyuki Nohira [a,b,*], Rika Hagiwara [a,b,*], Atsushi Fukunaga [c], Koma Numata [c], Eiko Itani [c], Shoichiro Sakai [c], Koji Nitta [c], Shinji Inazawa [c]

[a] Graduate School of Energy Science, Kyoto University, Yoshida Sakyo-ku, Kyoto 606–8501, Japan
[b] Unit of Elements Strategy Initiative for Catalysts & Batteries (ESICB), Kyoto University, Katsura, Kyoto 615-8510, Japan
[c] Sumitomo Electric Industries Ltd., 1-1-3 Shimaya, Konohana-ku, Osaka 554-0024, Japan

HIGHLIGHTS

- The Na[FSA]–[C_2C_1im][FSA] ionic liquids are examined as electrolyte for Na secondary batteries.
- The liquid state is observed in a wide composition range of Na[FSA].
- The ionic conductivities are reasonably high even at a high Na[FSA] fraction.
- Stable Na metal deposition/dissolution occurs in the present hybrid ionic liquid at 363 K.

ARTICLE INFO

Article history:
Received 14 March 2014
Received in revised form
22 April 2014
Accepted 22 April 2014
Available online 2 May 2014

Keywords:
Ionic liquid
Sodium secondary battery
Imidazolium
Electrodeposition
Sodium metal

ABSTRACT

Physical and electrochemical properties of the Na[FSA]–[C_2C_1im][FSA] ($C_2C_1im^+$:1-ethyl-3-methylimidazolium and FSA^-:bis(fluorosulfonyl)amide) ionic liquids have been investigated in view of their application as electrolytes for sodium secondary batteries operating in a wide temperature range. The Na[FSA]–[C_2C_1im][FSA] ionic liquids in the range of $0.0 \leq x(\mathrm{Na[FSA]}) \leq 0.5$ are in the liquid state at room temperature, where x(Na[FSA]) is the mole fraction of Na[FSA]. In the case of $x(\mathrm{Na[FSA]}) = 0.3$, the ionic conductivity, viscosity, and electrochemical window at 298 K are 5.4 mS cm^{-1}, 78 mPa s, and 5.1 V, respectively. Sodium metal deposition/dissolution test in the ionic liquid at $x(\mathrm{Na[FSA]}) = 0.3$ resulted in average cycle efficiencies of 69% and 96% at 298 K and 363 K, respectively, at a current density of 1.0 mA cm^{-2}.

1. Introduction

Sodium secondary batteries are interesting candidates as energy storage devices for stationary use and electric vehicles owing to high abundance and low cost of sodium resources as well as the low Na/Na^+ redox potential [1]. Various candidates of negative and positive electrodes have been explored in the last three years [1], whereas only limited numbers of electrolytes are available so far. Although the organic solutions, usually carbonates, of a Na salt such as $Na[ClO_4]$ and $Na[PF_6]$ are widely used in Na secondary batteries [2–4], ionic liquids are attractive electrolyte candidates to improve safety issues and to widen operation temperature [5–9] owing to their unique properties including low vapor pressure, low flammability, and wide liquid temperature range [10–12]. We have demonstrated sodium secondary batteries using bis(fluorosulfonyl)amide anion (FSA)-based ionic liquids show good performance with the Sn–Na alloy negative electrode and $NaCrO_2$ and $Na_2FeP_2O_7$ positive electrodes in an inorganic FSA ionic liquid, Na[FSA]–K[FSA], at 363 K [6–8] and in an inorganic–organic hybrid FSA ionic liquid, Na[FSA]–[C_3C_1pyrr][FSA] (C_3C_1pyrr:*N*-methyl-*N*-propylpyrrolidinium), at 298–358 K [13].

* Corresponding authors. Unit of Elements Strategy Initiative for Catalysts & Batteries (ESICB), Kyoto University, Katsura, Kyoto 615-8510, Japan. Tel.: +81 75 753 5822; fax: +81 75 753 5906.
E-mail addresses: nohira@energy.kyoto-u.ac.jp (T. Nohira), hagiwara@energy.kyoto-u.ac.jp (R. Hagiwara).

http://dx.doi.org/10.1016/j.jpowsour.2014.04.112
0378-7753/

In such studies on Na secondary batteries, only a few examples using imidazolium-based ionic liquid electrolytes are available in spite of their high ionic conductivities. This may arise from the fact that imidazolium-based ionic liquids are able to be used as electrolytes for Li secondary batteries only in limited situations [14–16]. For example, practically acceptable ionic conductivity and viscosity were recently reported for the Na[TFSA]-[C_2C_1im][TFSA] (C_2C_1im:1-ethyl-3-methylimidazolium and TFSA:bis(trifluoromethylsulfonyl)amide) ionic liquids [17]. The present study shows the high potential of [C_2C_1im][FSA]-based ionic liquids as electrolytes for Na secondary batteries with high ionic conductivities and wide liquid temperature ranges.

2. Experimental

Air sensitive materials were handled in a glovebox under a dried and deoxygenated argon atmosphere. The Na[FSA] salt (Mitsubishi Materials Electronic Chemicals Co., Ltd., water content < 72 ppm) was dried under vacuum at 353 K prior to use. The room temperature ionic liquid, [C_2C_1im][FSA] (Kanto Chemical Co., Ltd., water content < 28 ppm), was used as purchased.

Phase transition temperatures for various compositions of Na[FSA]–[C_2C_1im][FSA] mixtures were determined by differential scanning calorimetry (DSC) (DSC-60, Shimadzu Corp.) at a scan rate of 5 K min^{-1} under a dry argon atmosphere. Samples were sealed in stainless steel cells in the glovebox and the measurements were performed under a dry Ar flow. Viscosities were measured by a cone and plate rheometer, LVDV-II+PRO (Brookfield Engineering Laboratories, Inc.). Ionic conductivities were measured with the aid of an impedance analyzer 3532-80 (Hioki E.E. Corp.) by an AC impedance technique using a cell with stainless steel disk electrodes. Water content was measured by Karl–Fischer titration (899 Coulometer, Metrohm). Density was measured using an oscillating U-tube density meter (DMA 4500 M, Anton Paar GmbH).

Cyclic voltammetry was performed with the aid of a Biologic VSP-300 system. The Na deposition/dissolution test was performed in a two-electrode cell at a current density of 1.0 mA cm^{-2} using a Hokuto Denko HJ1001SD8 system. Sodium metal of 1.0 C cm^{-2} was first deposited on a Cu substrate and Na dissolution and deposition of 0.2 C cm^{-2} were repeated until the electrode potential reached 0.5 V vs. Na/Na^+ during the dissolution.

3. Results and discussion

Table 1 lists selected physical properties of the Na[FSA]–[C_2C_1im][FSA] ionic liquids. Fig. 1 shows the Na[FSA]–[C_2C_1im][FSA] phase diagram based on the DSC measurements (see Supplementary data for the DSC curves). Thermal behavior of [C_2C_1im][FSA] and Na[FSA] single salts is in good agreement with previous reports [14,15,18]. In the range of $0.3 \leq x$(Na[FSA]) ≤ 0.5, where x(Na[FSA]) denotes mole fraction of Na[FSA], melting of the crystal phase disappears and only glass transition is observed in the present DSC measurements. Although the salts in the range of $0.0 \leq x$(Na[FSA]) ≤ 0.5 are certainly liquid at room temperature, very slow transitions below room temperature may not be detectable by the present DSC study. For example, the salt at x(Na[FSA]) = 0.5 did not crystallize after aging at 243 K for 24 h but did after 3 weeks. The [$C_nC_1$im][TFSA]–Li[TFSA] ($C_nC_1$im:1-alkyl-3-methylimidazolium with n = 2, 3, and 4) system shows similar behavior (disappearance of melting from crystal phases) in a wide Li[TFSA] range [19], whereas the binary systems of alkali metal FSA salts [20] and the [$C_nC_1$pyrr][TFSA]–Li[TFSA] ($C_nC_1$pyrr:*N*-alkyl-*N*-methylpyrrolidinium with n = 2, 3, and 4) system [21] exhibit crystallization at any composition. The solid–solid transition, which was reported for the Na[FSA] single salt (375 K) [18], is also observed at x(Na[FSA]) = 0.8 and 0.9. Glass transition temperature increases with increase in x(Na[FSA]) and becomes nearly constant in the range of $0.6 \leq x$(Na[FSA]) ≤ 0.8. Similar trend was observed for the Na[TFSA]–[C_2C_1im][TFSA] [17], the Li[TFSA]–[C_4C_1pyrr][TFSA] (C_4C_1pyrr:*N*-butyl-*N*-methylpyrrolidinium) [22], and the [$C_nC_1$pyrr][TFSA]-Li[TFSA] ($C_nC_1$pyrr:*N*-alkyl-*N*-methylpyrrolidinium with n = 2, 3, and 4) systems [21]. According to this phase diagram, a wide liquid temperature range more than 100 K around room temperature is achieved in the composition range of $0.0 \leq x$(Na[FSA]) ≤ 0.5. The combination of $C_2C_1im^+$ and FSA^- that tend to form low melting salts probably contributes to this behavior.

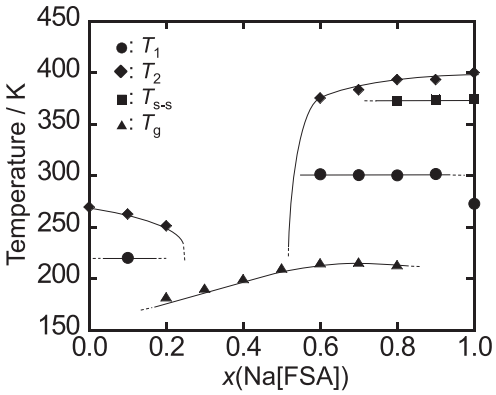

Fig. 1. Phase diagram of the Na[FSA]–[C_2C_1im][FSA] system based on the DSC transition temperatures in Table 1 (T_1: the onset temperature of melting, T_2: the end temperature of melting: T_{s-s}: solid–solid transition temperature, and T_g: glass transition temperature).

Table 1
Selected physical properties of the Na[FSA]–[C_2C_1im][FSA] ionic liquids.[a]

x(Na[FSA])	T_1/K	T_2/K	T_{s-s}/K	T_g/K	ρ/g cm^{-3}	σ/mS cm^{-1}	η/mPa s
0.0	260	269	n.d.	n.d.	1.442	16.6	20.3
0.1	249	263	n.d.	n.d.	1.478	12.2	28.9
0.2	n.d.	251	n.d.	182	1.519	8.5	43.4
0.3	n.d.	n.d.	n.d.	191	1.561	5.4	78.0
0.4	n.d.	n.d.	n.d.	200	1.612	2.9	157.8
0.5	n.d.	n.d.	n.d.	210	1.664	1.2	343.7
0.6	302	376	n.d.	215	–	–	–
0.7	301	384	n.d.	216	–	–	–
0.8	301	394	373	214	–	–	–
0.9	302	394	374	n.d.	–	–	–
1.0	391	401	375	n.d.	–	–	–

[a] T_1: the onset temperature of melting, T_2: the end temperature of melting, T_{s-s}: solid–solid transition temperature, T_g: glass transition temperature, ρ: density at 298 K, σ: ionic conductivity at 298 K, η: viscosity at 298 K, and n.d.: not detected. The T_1, T_2, T_{s-s}, and T_g values were determined based on the DSC analysis at a scan rate of 5 K min^{-1}.

Fig. 2 shows Arrhenius plots of viscosity and ionic conductivity for the Na[FSA]–[C_2C_1im][FSA] ionic liquids of x(Na[FSA]) = 0, 0.1, 0.2, 0.3, 0.4 and 0.5. The present ionic conductivity of the [C_2C_1im][FSA] single salt (16.6 mS cm^{-1}) is in good agreement with previously reported values (16.5 mS cm^{-1} [14] and 15.4 mS cm^{-1} [15]). The plots have concave and convex shapes for the viscosities and ionic conductivities, respectively, in the temperature range of measurement. This behavior is typical for ionic liquids and the Vogel–Tamman–Fulcher (VTF) equation [23,24] (Eqs. (1) and(2)) is known to fit such behavior better than the Arrhenius equation [25,26]:

$$\eta = A_\eta T^{1/2} \exp\left[B_\eta/(T - T_{0\eta})\right] \quad (1)$$

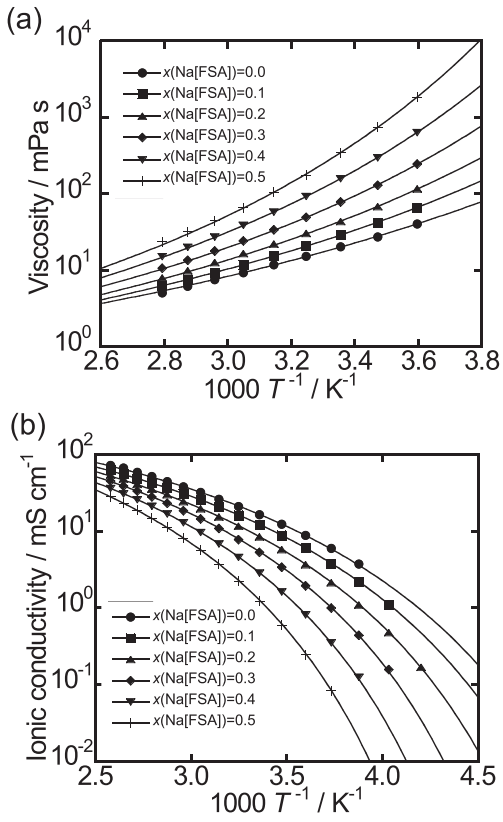

Fig. 2. Arrhenius plots of (a) viscosity and (b) ionic conductivity for the Na[FSA]–[C_2C_1im][FSA] (x(Na[FSA]) = 0.0, 0.1, 0.2, 0.3, 0.4, and 0.5) ionic liquids.

$$\sigma = A_\sigma T^{-1/2} \exp[-B_\sigma/(T - T_{0\sigma})] \quad (2)$$

where η and σ are viscosity and ionic conductivity, respectively, and A_η, B_η, $T_{0\eta}$, A_σ, B_σ, and $T_{0\sigma}$ are VTF parameters as shown in Table 2. Although the $T_{0\eta}$ and $T_{0\sigma}$ values, called ideal glass transition temperatures, are lower than the observed T_g values, their trends against x(Na[FSA]) match that of the observed T_g in Fig. 1. The B_η and B_σ parameters, which are related with activation energies, increase with increase in x(Na[FSA]) as is reflected in the gradients of the plots in the high temperature range. The A_η and A_σ parameters increases and decreases, respectively, with increase in x(Na[FSA]). The ionic conductivity at 298 K monotonously decreases with increase in x(Na[FSA]) from 16.6 mS cm^{-1} for x(Na[FSA]) = 0.0 to 1.23 mS cm^{-1} for x(Na[FSA]) = 0.5. The ionic conductivities of the present ionic liquids are higher than those of the ionic liquid electrolytes of the same composition and temperature previously investigated for Na and Li secondary batteries owing to the low viscosity of FSA-based ionic liquids (for instance, 3.2 mS cm^{-1} for Na[FSA]–[C_3C_1pyrr][FSA] at x(Na[FSA]) = 0.2 at 298 K, [13], 10.6 mS cm^{-1} for Li[TFSA]–[C_2C_1im][TFSA] at x(Li[TFSA] = 0.11) at 303 K [27], and 11.0 mS cm^{-1} for Li[TFSA]–[C_2C_1im][FSA] at x(Li[TFSA] = 0.08) at 298 K) [15].

Table 2
The VTF parameters of viscosity and ionic conductivity for the Na[FSA]–[C_2C_1im][FSA] ionic liquids.[a]

x(Na[FSA])	10^3A_η/mPa s $K^{-1/2}$	B_η/K	$T_{0\eta}$/K	$10^{-4}A_\sigma$/mS cm^{-1} $K^{1/2}$	B_σ/K	$T_{0\sigma}$/K
0.0	5.86	865	134	1.70	579	156
0.1	5.30	877	145	1.74	608	160
0.2	4.76	912	153	1.75	623	167
0.3	4.68	931	162	1.77	632	177
0.4	3.94	995	170	2.07	684	184
0.5	3.39	1054	177	2.55	752	191

[a] The symbols, A_η, B_η, $T_{0\eta}$, A_σ, B_σ, and $T_{0\sigma}$, are the VTF parameters in Eqs. (1) and (2) and determined from the plots in Fig. 1.

Fig. 3 shows a combined cyclic voltammogram of Cu disk (negative potential region), glassy carbon disk (positive potential region), and Al plate (positive potential region) electrodes in the Na[FSA]–[C_2C_1im][FSA] ionic liquid at x(Na[FSA]) = 0.3 at 298 K. The cathodic and anodic currents observed around 0 V vs. Na/Na^+ correspond to electrodeposition and electrodissolution of Na metal, respectively. Dendritic deposition of Na metal was visually confirmed during and after electrochemical measurements. No sign of the decomposition of $C_2C_1im^+$ is observed during the cathodic scan. This stands in contrast to the case of Li metal deposition in $C_2C_1im^+$-based ionic liquids [28], which suffers from the cathodic instability of $C_2C_1im^+$. Due to the higher redox potential of sodium than that of lithium, stable and reversible deposition and dissolution of sodium is realized in this system. The stable Na deposition/dissolution indicates the high performance of the Na[FSA]–[C_2C_1im][FSA] ionic liquids as electrolytes for sodium secondary batteries. The anodic limit on a glassy carbon electrode is determined to be 5.1 V (anodic current density of 0.5 mA cm^{-2}). The Al working electrode exhibits a high anodic stability in this ionic liquid probably owing to the formation of passivation film as in the case of the Al electrode in many organic solvents, suggesting the validity of use of an Al current collector for positive electrodes for sodium secondary batteries.

Sodium deposition/dissolution test was performed at the current density of 1.0 mA cm^{-1} in the Na[FSA]–[C_2C_1im][FSA] ionic liquid at x(Na[FSA]) = 0.3 at 298 K using a Cu working electrode and a Na counter electrode. The average cycle efficiency of Na deposition/dissolution (ε_{cycle}) is obtained according to the following equation (Eq. (3)):

$$\varepsilon_{cycle} = N_{eff} \cdot Q_{cycle} \Big/ \left(Q_{ex} + N_{eff} \cdot Q_{cycle}\right) \quad (3)$$

where N_{eff} is cycle number until the electrode potential reached 0.5 V vs. Na/Na^+, Q_{cycle} is the electric charge for Na deposition/dissolution (0.2 C cm^{-2}), and Q_{ex} is the extra amount of electricity theoretically not necessary (0.8 C cm^{-2}). The test at 298 K continued for 9 cycles, giving ε_{cycle} of 69%. By making use of good thermal stability of ionic liquids, the same test was performed at 363 K, because good electrochemical properties were already confirmed at this temperature in several FSA-based ionic liquids [6–8,13]. The ε_{cycle} value at 363 K was 96% for 93 cycles and is better

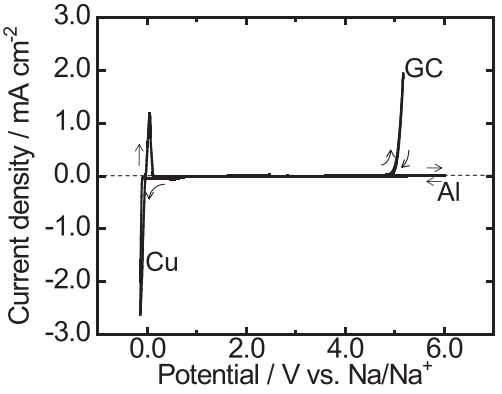

Fig. 3. A combined cyclic voltammogram of Cu disk (negative potential region), glassy carbon (GC) disk (positive potential region), and Al plate (positive potential region) electrodes in the Na[FSA]–[C_2C_1im][FSA] ionic liquid at x(Na[FSA]) = 0.3 at 298 K. Reference and counter electrodes are Na metal. Scan rate: 5 mV s^{-1}.

than that at 298 K. The higher ε_{cycle} value at 363 K is considered to arise from the suppression of dendritic Na metal deposition at the temperature near the melting point of Na metal (371 K) because diffusion of atoms at metal surface becomes faster near the melting point. Decrease in viscosity and increase in ionic conductivity by the elevation of temperature (78.0 mPa s and 5.4 mS cm^{-1} at 298 K and 9.1 mPa s and 31.1 mS cm^{-1} at 363 K) accelerate the supply of Na^+ to the electrode and may also suppress the dendritic Na metal deposition. One of the possible factors to decrease ε_{cycle}, the reaction of the deposited Na metal with impurities in the ionic liquid or with the ionic liquid itself, is considered to be ruled out in this case because such a reaction to decrease ε_{cycle} should be accelerated at elevated temperatures, which contradicts the present observations.

4. Conclusion

This study reported physical and electrochemical properties of the Na[FSA]–[C_2C_1im][FSA] ionic liquids. A wide temperature range more than 100 K around room temperature is achieved in the composition range of $0.0 \leq$ Na[FSA] ≤ 0.5. The ionic conductivities of these Na-containing ionic liquids are higher than known ionic liquid electrolytes at the same composition of Na salt. The electrochemical window is 5.1 V and stable electrodeposition and electrodissolution of Na metal occurs around 0 V vs. Na/Na^+ for x(Na[FSA]) = 0.3 at 298 K. The wide electrochemical window enables the use of various positive electrode materials. These results suggest the high potential of these ionic liquids as electrolytes for Na secondary batteries.

Acknowledgments

This work was performed under a management of 'Elements Strategy Initiative for Catalysts & Batteries (ESICB)' supported by Ministry of Education, Culture, Sports, Science, and Technology, Japan (MEXT).

Appendix A. Supplementary data

Supplementary data related to this article can be found at http://dx.doi.org/10.1016/j.jpowsour.2014.04.112.

References

[1] H.L. Pan, Y.S. Hu, L.Q. Chen, Energy Environ. Sci. 6 (2013) 2338–2360.
[2] A. Ponrouch, R. Dedryvere, D. Monti, A.E. Demet, J.M.A. Mba, L. Croguennec, C. Masquelier, P. Johansson, M.R. Palacin, Energy Environ. Sci. 6 (2013) 2361–2369.
[3] K. Kuratani, N. Uemura, H. Senoh, H.T. Takeshita, T. Kiyobayashi, J. Power Sources 223 (2013) 175–182.
[4] Z.L. Jian, W.Z. Han, X. Lu, H.X. Yang, Y.S. Hu, J. Zhou, Z.B. Zhou, J.Q. Li, W. Chen, D.F. Chen, L.Q. Chen, Adv. Energy. Mater. 3 (2013) 156–160.
[5] S.A.M. Noor, P.C. Howlett, D.R. MacFarlane, M. Forsyth, Electrochim. Acta 114 (2013) 766–771.
[6] C.Y. Chen, K. Matsumoto, T. Nohira, R. Hagiwara, A. Fukunaga, S. Sakai, K. Nitta, S. Inazawa, J. Power Sources 237 (2013) 52–57.
[7] T. Yamamoto, T. Nohira, R. Hagiwara, A. Fukunaga, S. Sakai, K. Nitta, S. Inazawa, J. Power Sources 217 (2012) 479–484.
[8] C.Y. Chen, K. Matsumoto, T. Nohira, R. Hagiwara, A. Fukunaga, S. Sakai, K. Nitta, S. Inazawa, J. Power Sources 246 (2014) 758–763.
[9] L.G. Chagas, D. Buchholz, L.M. Wu, B. Vortmann, S. Passerini, J. Power Sources 247 (2014) 377–383.
[10] H. Ohno, Electrochemical Aspects of Ionic Liquids, second ed., John Wiley & Sons Inc., Hoboken, New Jersey, 2011.
[11] J.P. Hallett, T. Welton, Chem. Rev. 111 (2011) 3508–3576.
[12] D.R. Macfarlane, M. Forsyth, P.C. Howlett, J.M. Pringle, J. Sun, G. Annat, W. Neil, E.I. Izgorodina, Acc. Chem. Res. 40 (2007) 1165–1173.
[13] C.S. Ding, T. Nohira, K. Kuroda, R. Hagiwara, A. Fukunaga, S. Sakai, K. Nitta, S. Inazawa, J. Power Sources 238 (2013) 296–300.
[14] M. Ishikawa, T. Sugimoto, M. Kikuta, E. Ishiko, M. Kono, J. Power Sources 162 (2006) 658–662.
[15] H. Matsumoto, H. Sakaebe, K. Tatsumi, M. Kikuta, E. Ishiko, M. Kono, J. Power Sources 160 (2006) 1308–1313.
[16] H. Matsumoto, H. Sakaebe, K. Tatsumi, J. Power Sources 146 (2005) 45–50.
[17] D. Monti, E. Jonsson, M.R. Palacin, P. Johansson, J. Power Sources 245 (2014) 630–636.
[18] K. Matsumoto, T. Oka, T. Nohira, R. Hagiwara, Inorg. Chem. 52 (2013) 568–576.
[19] Q. Zhou, K. Fitzgerald, P.D. Boyle, W.A. Henderson, Chem. Mater. 22 (2010) 1203–1208.
[20] K. Kubota, T. Nohira, R. Hagiwara, J. Chem. Eng. Data 55 (2010) 3142–3146.
[21] W.A. Henderson, S. Passerini, Chem. Mater. 16 (2004) 2881–2885.
[22] A. Martinelli, A. Matic, P. Jacobsson, L. Borjesson, A. Fernicola, B. Scrosati, J. Phys. Chem. B 113 (2009) 11247–11251.
[23] H. Vogel, Phys. Z 22 (1921) 645–646.
[24] G.S. Fulcher, J. Am. Ceram. Soc. 8 (1925) 339–355.
[25] H. Tokuda, K. Hayamizu, K. Ishii, M. Abu Bin Hasan Susan, M. Watanabe, J. Phys. Chem. B 108 (2004) 16593–16600.
[26] A. Noda, K. Hayamizu, M. Watanabe, J. Phys. Chem. B 105 (2001) 4603–4610.
[27] S. Seki, Y. Kobayashi, H. Miyashiro, Y. Ohno, A. Usami, Y. Mita, N. Kihira, M. Watanabe, N. Terada, J. Phys. Chem. B 110 (2006).
[28] H. Matsumoto, M. Yanagida, K. Tanimoto, M. Nomura, Y. Kitagawa, Y. Miyazaki, Chem. Lett. (2000) 922–923.